Hindawi
International Journal of Chemical Engineering
Volume 2022, Article ID 7254646, 10 pages
https://doi.org/10.1155/2022/7254646

Research Article

Methodological Approach for Optimizing Production of Oxygen by Adsorption of Nitrogen from Air using Zeolite Li-LSX

Marwa Al-Yousuf[1], **Raghad F. Almilly**[1] **and Riyadh Kamil**[2]

[1]*Chemical Engineering Department, University of Baghdad, Baghdad, Iraq*
[2]*Petroleum and Petrochemical Research Center, Ministry of Science and Technology (MoST), Baghdad, Iraq*

Correspondence should be addressed to Marwa Al-Yousuf; marwa.ali1607m@coeng.uobaghdad.edu.iq

Received 6 August 2022; Revised 11 September 2022; Accepted 16 September 2022; Published 29 October 2022

Academic Editor: Selvaraju Narayanasamy

This research investigates the optimum operating conditions related to the adsorption of nitrogen gas from ambient air on zeolite Li-LSX to produce oxygen gas by the pressure-vacuum swing adsorption process. Experiments were performed using a column (4 cm inside diameter and 17 cm length) packed with different heights of packing (h) of zeolite (9, 12, and 16 cm) from 0.4 to 0.8 mm diameter pellets. At each packing height, different flow rates (f) (2, 4, 6, 8, and 10 L·min^{-1}) for different input pressures (p) (0.5, 1, 1.5, 2, and 2.5 bar) were used to detect their effects on the purity of produced oxygen as percentage volume of the outlet air stream. The results showed that the purity of produced oxygen increased with increasing packing height, pressure, and flowrate to a specific limit. The maximum purity obtained was 73.15% at 16 cm packing height, 2.5 bar input pressure, and 6 L·min^{-1} inlet flowrate, and the productivity was equal to 18 mmol·(Kg·s)$^{-1}$ at these conditions. A response surface methodology was used to determine the most influential variables and their interactions. The results confirmed the strong effects of the input pressure, the packing height, and to a lesser extent, the flowrate. A quadratic model was predicted based on the experimental result and assessed statistically. The impacts of quadratic terms in the model were in the order: of $p * p > p * h > p * f$. The model was applied to predict the operating conditions of 95% purity of oxygen.

1. Introduction

Because of the COVID-19 pandemic, the demand for portable medical oxygen has gone through the roof [1]. COVID-19, chronic obstructive pulmonary disease (COPD), chronic bronchitis, and pneumonia all need medical oxygen concentrators (MOCs) to avoid hypoxemia-related problems [1–4]. The World Health Organization says that everyone should get oxygen therapy [1]. Three basic technologies are used to separate air into its constituents (i.e., oxygen and nitrogen): adsorption, membrane, and cryogenic separation [5]. The amount of separation products needed often determines how useful each technology is [6]. The adsorption separation method is used to produce oxygen that is very pure [7]. Based on this, many pieces of medical oxygen equipment have been made [2]. Adsorption is used to separate the air components according to their different sorption abilities [8]. N_2-selective adsorbents are often used, such as zeolites, to produce pure oxygen. For modified zeolites like Li-LSX, the selectivity for N_2 adsorption is low. It increased as a result of the interaction between the dipole and quadrupole moments of the guest gas molecules and the additional frame cations of zeolites [9]. There are several modes of adsorption operation, such as pressure swing (PSA), vacuum swing (VSA), or pressure-vacuum swing adsorption processes (PVSA) [1, 10]. Compared to the temperature swing adsorption (TSA) process cycle, the PSA process cycle usually takes between one and several seconds, while the TSA method takes hours. Therefore, PSA is the method most often used, [2] and the most beneficial way to separate gases is the PVSA process, in which the adsorption step takes place at pressures above the atmospheric, and the regeneration of the adsorbent takes place under vacuum pressure [11]. In comparing the PVSA

and PSA processes, the results show that the PVSA process has a higher purity and recovery rate of O_2/N_2 than the PSA process. Gas from light- and heavy-reflux streams are reproduced, which explains why PVSA's adsorbent productivity is higher than PSA's. This means that PVSA's processing capacity and adsorbent productivity are more elevated than PSA's [9]. The PVSA process uses less energy than the PSA process with the total energy use because the vacuum pump consumes far less energy than a conventional pump. The light and heavy component mass transfer zones often interfere in a formal dual-reflux PSA process with an intermediate feed. The PVSA processes offer the right way to solve this problem. The mass transfer zone and adsorbent use rate are significantly improved using an integrated PVSA process [12]. The feasibility of PVSA of N_2 to produce pure O_2 can be determined by estimating the productivity, which is defined by equation (1) [3]:

$$\text{Productivity} = \frac{\textbf{Moles of } O_2}{(\textbf{time} \times \textbf{adsorbent mass})}. \quad (1)$$

The objective of the present work is to find a model based on experiments to represent the process of producing oxygen from air by adsorbing nitrogen and relate the three effective variables, i.e., input pressure, packing height, and the inlet air flow rate by a mathematical relationship. Moreover, using the predicted model to optimize the process and to be able to scale up the system without the need for more experiments.

2. Experimental Work

2.1. Materials. The material used in the experiment is Zeolite Li-LSX branched from China, and its technical specification of it is listed in Table 1.

2.2. Equipment. The experimental setup is shown in Figure 1. All the equipment used is listed in Table 2. Figure 2 shows the schematic diagram of the experiment setup.

2.3. Procedure. The adsorbent preparation included heating zeolite in the oven at 110℃ for 45 minutes to get rid of moisture and other impurities before stuffing it in the column. Then, the helium gas was passed over the packing to refresh it for adsorption. The air compressor was turned on to get the desired input pressure. Then, the drum was filled with air to keep its flow stable during the experiment. The inlet air was passed through a silica gel-filled filter to remove the moisture and pollutants [13]. The flow meter was set to a specified flow rate. When the air was pushed through the zeolite packing, nitrogen gas was adsorbed, leaving a stream of oxygen-rich gas. The produced stream was split into two streams: the first attached to the concentration sensor, which detected the presence of oxygen as a volume percent of the stream, and the second led to the storage cylinder. There was a desorption process that completed one cycle of operation after each adsorption process. The desorption process was necessary to regenerate the zeolite by inducing vacuum pressure through the bed at −0.9 bar for 2 minutes to remove N_2 molecules from the zeolite surface [14].

Table 1: The technical specification of zeolite Li-LSX (commercial name JLOX-101).

Property	Unit	JLOX-101
Diameter	mm	0.4–0.8
N_2 adsorption capacity	$Ml{\cdot}g^{-1}$	≥ 22
N_2/O_2 selectivity	—	≥ 6.20
Crush strength	N	—
Bulk density	$g{\cdot}mL^{-1}$	0.63 ± 0.03
Moisture content	wt%	≤ 0.5
Particle ratio	%	≥ 95

2.4. Experimental Design. Response surface methodology (RSM) is a mix of statistical and mathematical methods that help to design, develop, and improve processes. This method can be used to figure out what the effects of different parameters are, how important they are, how they affect each other, and what the best conditions are for getting the responses that are needed. RSM is used in a lot of chemical engineering and applied science processes, like the adsorption process, to measure and optimize the effects of the operating parameters interacting with each other. In this study, a Box–Behnken Design (BBD) of experiments was used to find the best conditions for producing oxygen gas by adsorbing nitrogen gas from the air. A 3-level, 3-factor BBD was used to determine how the chosen parameters affected zeolite's ability to catch nitrogen out of the air [15]. Pressure (X_1), height of packing (X_2), and the flow rate (X_3) were chosen as the coded process variables, and the amount of oxygen that could be produced (Y) was chosen as the coded response.

The design has three levels: low, medium, and high, which are represented by the codes −1, 0, and +1. The variance in the data was calculated, and the regression coefficient (R^2) was calculated to determine the model's goodness of fit. Fifteen experimental runs were conducted under different combinations of pressure, height of packing, and the flowrate to identify which parameters and their interactions significantly impacted the purity of the produced oxygen [16]. Table 3 illustrates the measured values of the process operating variables and the response represented by the purity of the produced oxygen. Experimental data analysis was performed using the Minitab-19 software. The method of least squares (MLS), a multiple regression analysis technique, was used to fit the experimental data.

3. Results and Discussion

3.1. Response Surface Model Analysis for Adsorption Process. The complete experimental runs used to establish the BBD model are listed in Table 3. The experimental and the predicted responses were listed for comparison.

The predicted and experimental values of purity were very close. The BBD model suggested the empirical regression equation representing the relationship between the oxygen purity and the three operating variables in terms of coded units as given in the equation.

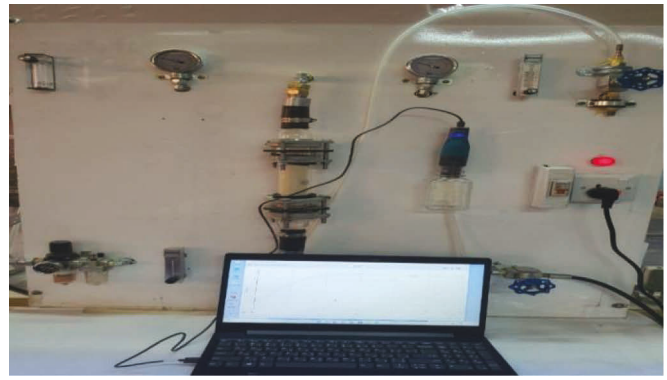

(a)

(b)

Figure 1: Photograph of experimental layout. (a): experimental setup. (b): compressor and drum.

Table 2: Equipment used in the research.

No.	Device	Specification	Range	Country
1	Air compressor	Ingco industrial 220–240 V, 50 Hz, AC25508	0–8 bar	China
2	Pressure gauge with filter unit	$D = 2.5$ cm $L = 5$ cm	0–10 bar	China
3	Feed flow meter	PMB CV.P. A10.LM. G2	1–10 L·min^{-1}	China
4	Adsorption column	Class type QVF $L = 17$ cm iD = 4 cm		
5	Product pressure gauge		0–3 bar	China
6	Product flow meter	PMB CV.P. A10.LM. G2	1–10 L·min^{-1}	China
7	O_2 gas sensor	GDX-O_2 $L = 15.5$ cm $D = 2.8$ cm	0–100% O_2	U. S.
8	Purge flow meter	Matheson U310	0.5–6 L·min^{-1}	China
9	Purge pressure gauge		0–3 bar	China
10	Valves			China
11	Drum	$L = 60$ cm $D = 37$ cm	V = 64479.9 cm^3	

$$Y = -19.7 - 8.54X_1 + 4.90X_2 + 4.95X_3 + 1.60X_1 * X_1 - 0.1270X_2 * X_2 - 0.2510X_3 * X_3 + 0.951X_1 * X_2 + 0.748X_1 * X_3 - 0.1440X_2 * X_3. \quad (2)$$

It was clear that the strong effect on the oxygen purity was due to input pressure. That was because increasing input pressure increased nitrogen adsorption from the air stream, leading to a high-volume percent of produced oxygen. This agreed with previous results [1–3]. The second variable that

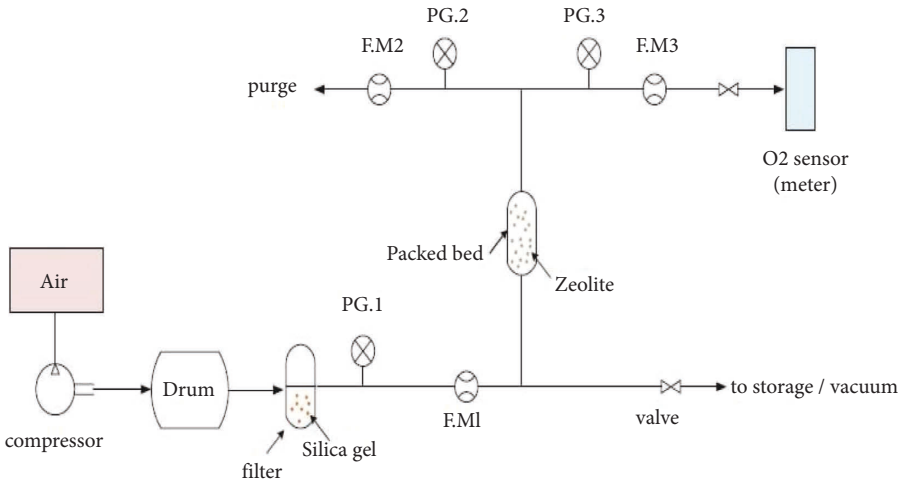

Figure 2: Schematic diagram of experiment setup.

Table 3: Experimental design of BBD for the production of oxygen.

Run	Pressure	Height	Flowrate	Actual purity	Predicted purity
1	1.5	16	2	44.98	46.3605
2	1.5	12	6	45.76	45.7600
3	0.5	12	10	34.41	33.4993
4	1.5	9	2	28.03	26.2949
5	2.5	12	2	46.30	47.2107
6	0.5	9	6	27.27	29.6407
7	2.5	16	6	73.15	70.9889
8	0.5	16	6	39.92	39.0161
9	1.5	9	10	41.73	40.4001
10	2.5	9	6	47.60	48.2943
11	1.5	12	6	45.76	45.7600
12	0.5	12	2	29.39	28.8339
13	2.5	12	10	63.29	63.8461
14	1.5	16	10	50.72	52.4045
15	1.5	12	6	45.76	45.7600

affected oxygen purity was the height of the packing, followed by the flowrate. The effect of the packing height, or precisely, the mass of zeolite available for adsorption, could be interpreted by considering that each particle offered an additional surface for adsorption. The flowrate was related to inducing turbulence, which had a significant role in renewing the zeolite surface available for adsorption. This occurred by the formation of eddies in the air stream, which swept out the nonadsorbed molecules from the zeolite surface constantly [17]. The quadratic terms of the model were in the order: $X_1 * X_1 X_1 * X_2 X_1 * X_3$. This indicated significant interactions between the variables. The most effective term was the quadratic effect of the pressure, followed by the interaction between the pressure and the packing height and, to a lesser extent, the pressure with the flowrate. The interactions refer to exaggerated effects (in the case of the quadratic pressure term $X_1 * X_1$) or counteracted effects between the variables (in the case of the product $X_1 * X_2$ and $X_1 * X_3$). The interaction between the variables implied an effect that might not be expected by simply adding the individual effects. The rest of the terms in the model seemed insignificant.

3.2. Statistical Analysis. The analysis of variance (ANOVA) was applied to evaluate the statistical appropriateness of the predicted model. ANOVA is a statistical method used to test the suppositions of the model coefficients by subdividing the total variance in a set of experimental data associated with a specific process into defined parts related to sources of variation [18]. The ANOVA analysis was determined based on the degree of freedom (DOF), (S) is a standard deviation, the sum of squares (SS), the adjusted mean of square (Adj. MS), the adjusted sum of squares (Adj. SS), *F*-value, and *P* -value. The ANOVA results are given in Table 4. In the ANOVA results table, the *F*-values and *P*-values showed how important each coefficient in the model was for the response. High significance was shown by high *F*-values and low *P*-values. The Fisher variation ratio (*F*-value) is the ratio of the mean square of the model (MS) to the appropriate error mean square. The greater the ratio, the greater the *F*-value, and the greater the probability that the model's variance is significantly greater than random. The probability value (*P*-value) is used to figure out which effects in the model are statistically important. If the *P*-value is less than 0.05, the effect of the coefficients is statistically significant with a 95% level of confidence [19]. The ANOVA results revealed that the *F*-value of 50.67 to produce oxygen was greater than the critical *F*-value for the significance level of 0.05, with freedom degrees equaling 9, which meant that the model was statistically significant. The *P*-value of 0.001 (0.05) indicated that the model was highly significant and could be used to predict adsorption process results [17].

The multiple correlation coefficient (R^2) was used to evaluate the goodness of model fitting. It was observed from Table 4 that the value of R^2 is 0.9892 showing that this regression was statistically significant, and the model did not explain only 1.08% of the total variance.

3.3. The Experimental and Predicted Effects of Variables. Figure 3 shows the effect of pressure on the purity of oxygen for different flowrates; the data are listed in Table 5. The purity was directly increased with pressure at all flowrates.

Table 4: Analysis of variance for production of oxygen.

Source	DF	SS	Adj SS	Adj MS	F-value	P-value
Model	9	2133.15	2133.15	237.02	50.67	0.001
Linear	3	1956.21	1983.91	661.30	141.37	0.001
X_1	1	1233.80	1268.70	1268.70	271.21	0.001
X_2	1	507.64	514.24	514.24	109.93	0.001
X_3	1	214.76	200.97	200.97	42.96	0.001
Square	3	79.90	79.90	26.63	5.69	0.045
$X_1 * X_1$	1	14.91	9.50	9.50	2.03	0.214
$X_2 * X_2$	1	5.43	8.50	8.50	1.82	0.236
$X_3 * X_3$	1	59.56	59.56	59.56	12.73	0.016
2-Way interaction	3	97.03	97.03	32.34	6.91	0.031
$X_1 * X_2$	1	44.80	44.80	44.80	9.58	0.027
$X_1 * X_3$	1	35.82	35.82	35.82	7.66	0.039
$X_2 * X_3$	1	16.41	16.41	16.41	3.51	0.120
Error	5	23.39	23.39	4.68		
Lack-of-Fit	3	23.39	23.39	7.80	*	*
Pure error	2	0.00	0.00	0.00		
Total	14	2156.54				
Model summary		S	R^2	R^2 (Adj.)	Press	R^2 (pred.)
		2.16285	98.92%	96.96%	389.110	81.96%

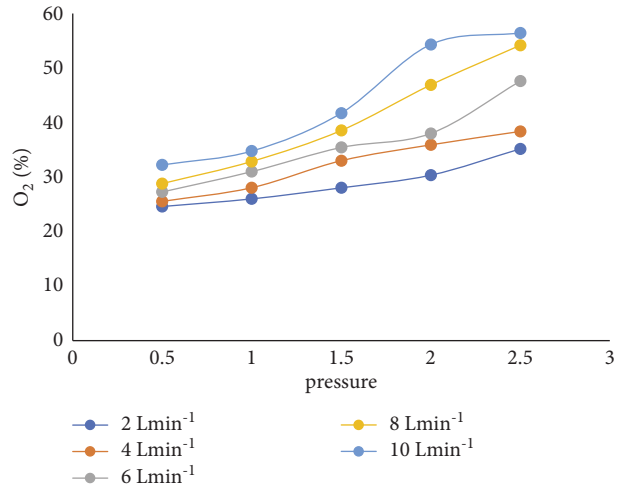

Figure 3: Oxygen purity as a function of pressure for different input air flowrates at 9 cm height of packing.

Table 5: Data of oxygen purity as a function of pressure for different input air flowrates at 9 cm height of packing.

pressure (bar)	2 L·min^{-1}	4 L·min^{-1}	6 L·min^{-1}	8 L·min^{-1}	10 L·min^{-1}
0.5	24.6	25.54	27.27	28.81	32.23
1	26	28.05	31	32.87	34.77
1.5	28.03	33	35.43	38.55	41.73
2	30.35	35.91	37.52	46.9	54.32
2.5	35.17	38.37	47.6	54.18	56.44

This was attributed to increasing the chance for molecules of the gas to access the pores on the zeolite surface. This effect was synergistically enhanced at high flowrates. The effect of flowrate on the purity of oxygen is illustrated in Figure 4. (Data for Figure 4 are available in Table S1 of the supplementary file).

Figure 4 shows that increasing the inlet air flowrate improved the adsorption process or oxygen purity while maintaining the previously discussed pressure and packing height constants.

Figure 5 shows the effect of packing height on the purity of oxygen along the time of the experiment (Data for Figure 4 are available in Table S1 in the supplementary file). It was clear that increasing bed height increased the purity. The maximum increase was observed in the first 20 s because of the high driving force for N_2 adsorption resulting from the empty sites on the solid. After about 50 s there was a drop in the oxygen purity due to filling the pores on the solid surface by adsorbed N_2 molecules and reaching an equilibrium state. Reaching equilibrium meant that the adsorption process stopped, and

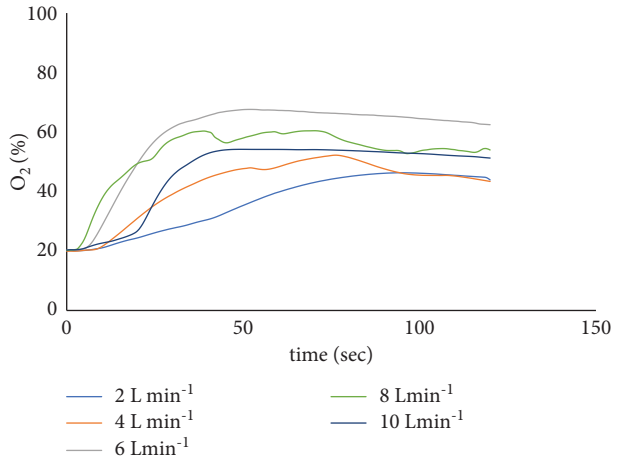

Figure 4: Oxygen purity as a function of time for different flowrates, input pressure 2.5 bar, and height of packing 9 cm.

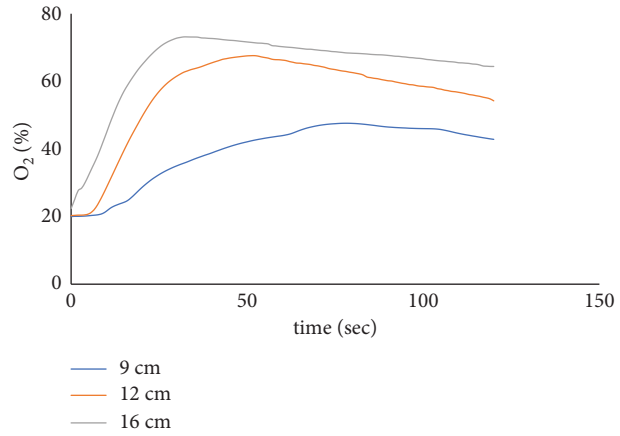

Figure 5: O_2% as a function of time for different heights of packing; input pressure 2.5 bar and inlet flow rate 6 L·min^{-1}.

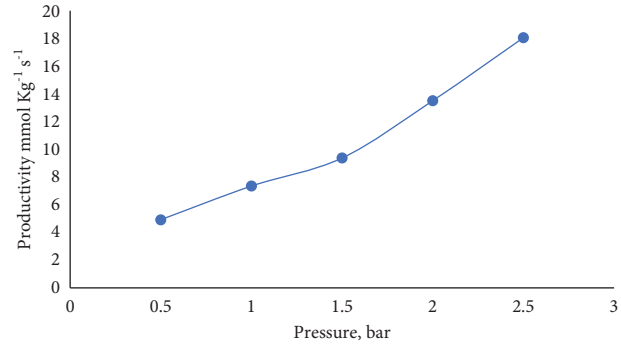

Figure 6: Effect of feed pressure on the productivity at 6 L·min^{-1} and 16 cm height of packing.

Table 6: Data of effect of feed pressure on the productivity at 6 L·min^{-1} and 16 cm height of packing.

Pressure (bar)	Time (s)	Productivity (mmol·(Kg·s)$^{-1}$)
0.5	40	4.9221
1	40	7.3484
1.5	50	9.3733
2	40	13.509
2.5	32	18.0530

the nitrogen molecules exited as they entered. Therefore, the purity or the volume percent of oxygen decreased. Another important point to discuss here is the undefined peak of maximum adsorption in the curve of 9 cm bed height. This indicated the fast reaching of equilibrium because of the low available sites for adsorption relative to the other bed heights.

Figure 6 shows the productivity as a function of input pressure. The curve is that as far as the pressure increased, the productivity of oxygen increased for a certain mass of packing. This indicated that increasing the operating costs would be only with the fixed cost unchanged. Here is an issue of optimization between increasing the pressure or increasing the packing mass that needs to study further for the purpose of scaling up. Optimum productivity was observed at 2.5 bar, 6 L·min^{-1} flow rate, and 16 cm height of packing (117.6016 g of zeolite) to be 18 mmol·(Kg·s)$^{-1}$. Data of Figure 6 are listed in Table 6. The time listed in the table is the time to reach equilibrium. The optimum productivity was acceptable in comparison with the published values [3].

The main effect plot can display the relationship between the response and the selected operating parameters. Figure 7 represents the main effect plot that illustrates the effects of the pressure, the height of packing, and flowrate on producing oxygen by applying the adsorption process. It was evident from the figure that the pressure had the main influence on the production, as also observed in the ANOVA analysis. It was observed from the main effect plot that the adsorption increased as the pressure increased from 0.5 to 2.5 bar, the height of packing increasing from 9 to 16 cm. The plot of flowrate showed curvature, indicating the existence of an optimum value within the range of study. This agrees with the experimental results.

The response surface and contour plots that show the interactive effects of the selected operating variables on the production of oxygen was depicted in Figure 8. The combined effects on the purity of oxygen were tested by varying X_1(pressure) from 0.5 to 2.5 bar, X_2 (Height of Packing) from 9 to 16 cm, and X_3 (Flowrate) from 2 to 10 L·min^{-1} to produce oxygen. As observed in the surface plot in Figure 8(a), there is a slight increase in the purity of oxygen with increasing the height and more increase with increased pressure at a flowrate of 6 L·min^{-1}. It is evident from the contour plot that the area of maximum values of O_2 purity is limited between the height (12.5–16 cm) and pressure (1.9–2.5 bar). Figure 8(b) explains that at any value of flowrate (2–10 L·min^{-1}), the purity of O_2 increases with increased pressure. It is evident from the contour plot that the area of maximum values of the purity of O_2 is confined between the flowrate value (6–10 L·min^{-1}) and pressure (2.3–2.5 bar). Figure 8(c) illustrates that there is a slight increase in the purity of oxygen with increasing the flowrate and more increase with an increase in height of packing at a constant pressure. It was clear from the contour plot that the area of maximum values of the purity of O_2 was confined between the flowrate value (3.5–10 L·min^{-1}) and height (13.5–16 cm).

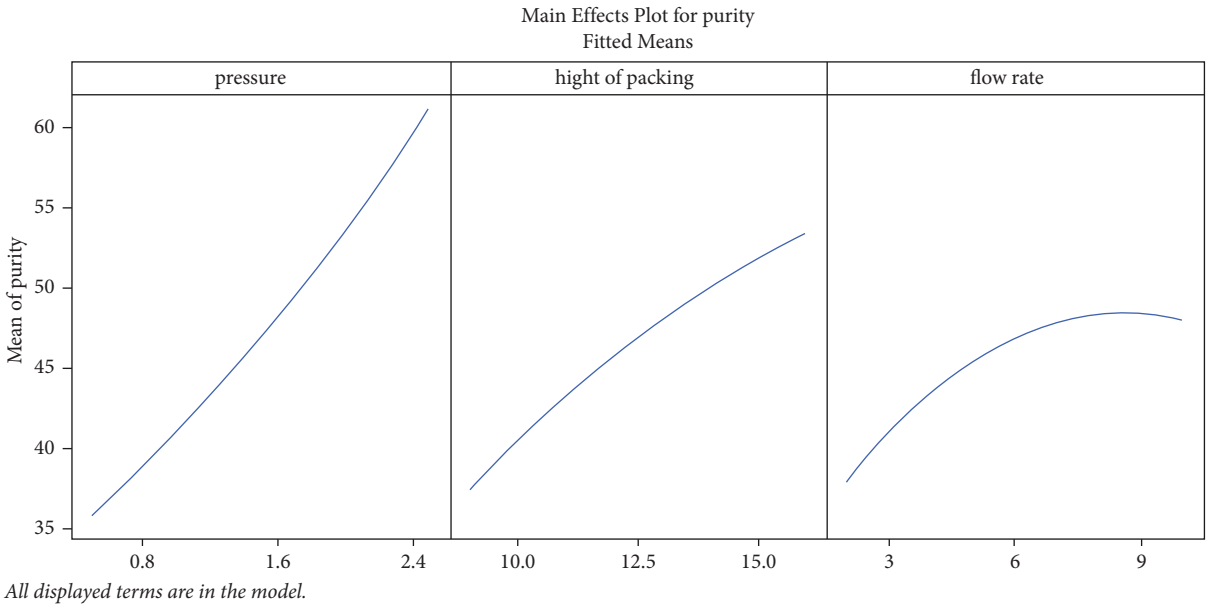

Figure 7: The predicted effects of process variables.

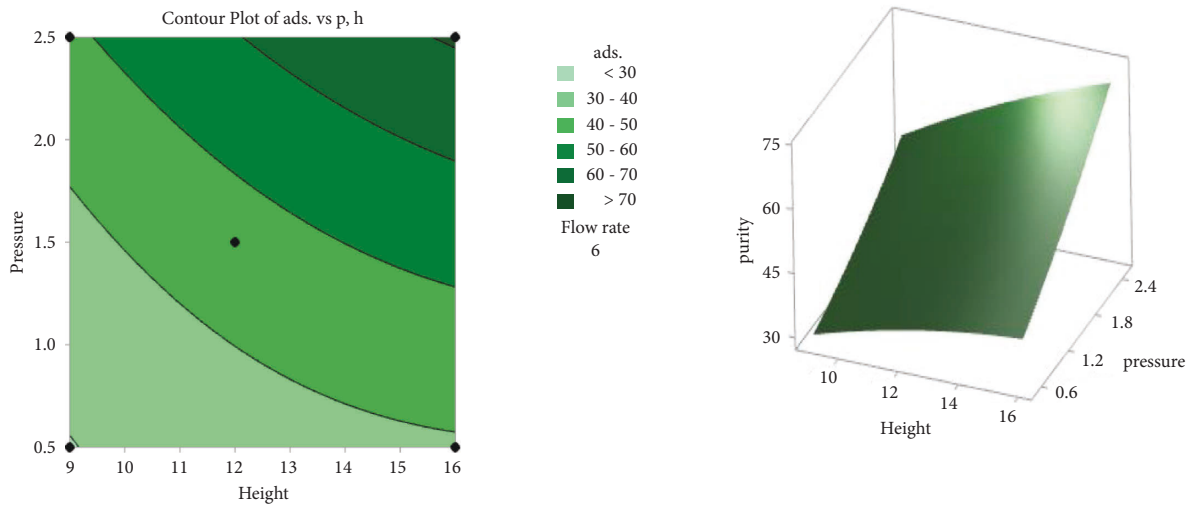

(a)

Figure 8: Continued.

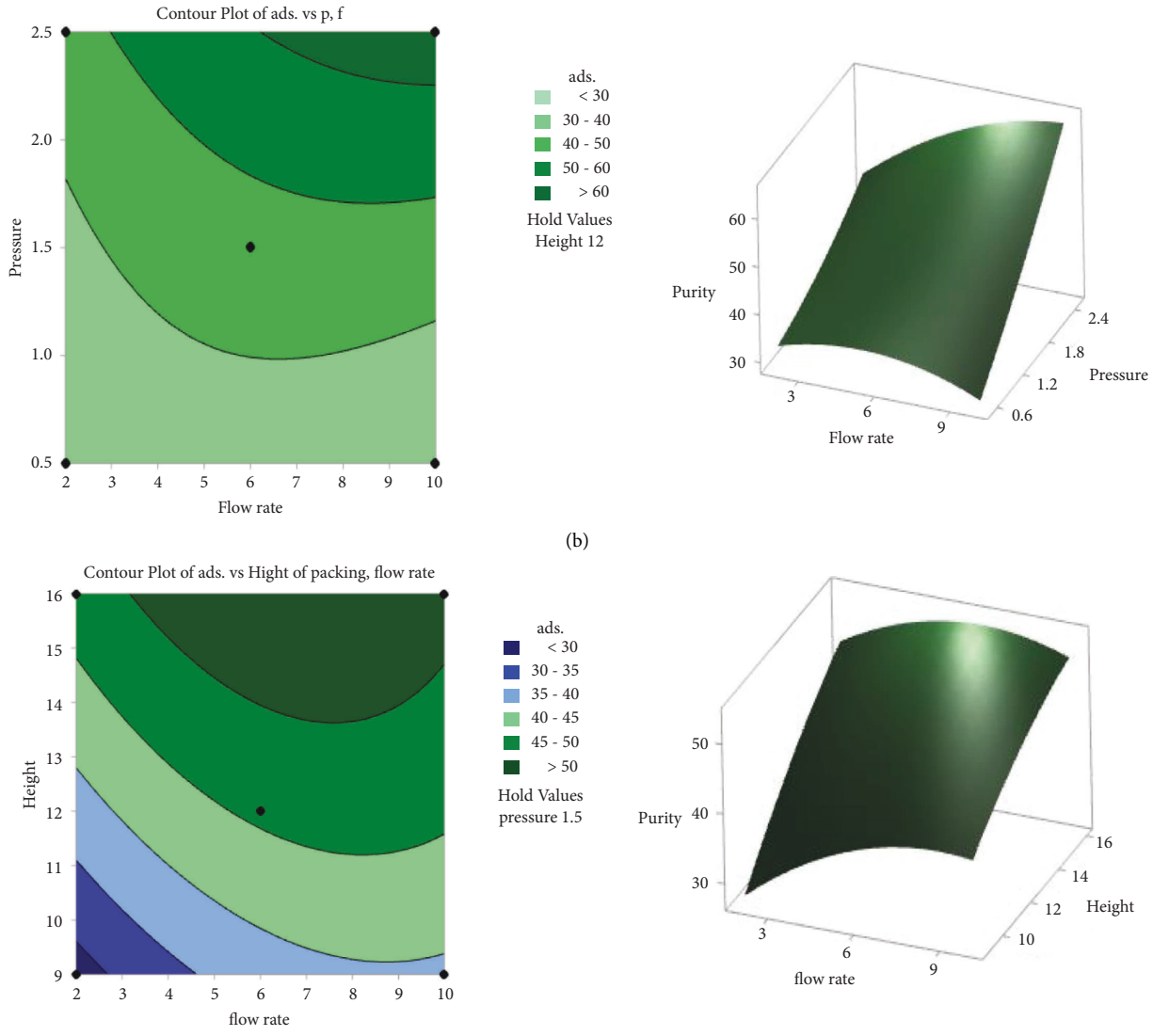

Figure 8: Response surface and contour plots for the effect of (a) pressure and height, (b) pressure and flowrate, and (c) height and flowrate on the purity of O_2.

Table 7: Optimal performance of the system.

Response	Goal	Lower	Target	Upper	Weight	Importance
% Purity	Maximum	27.27	95	104.5	1	1
			Solution and parameter			
Solution	Pressure		Flowrate	Height	Purity % fit	Composite desirability
1	2.5		9.0303	16	73.2403	0.678728
Response	Fit	SE fit	95% CI	95% PI		
% Purity	73.24	2.28	(67.39, 79.09)	(65.17, 81.31)		

Table 7 and Figure 9 show the optimization attained by applying the RSM regression equation. When optimizing the purity of oxygen from regarding goal fields, the selected operating variables of pressure (X_1), flowrate (X_2), and height of packing (X_3) were within the range of study and the result, namely, purity of oxygen (Y), was maximized with a corresponding weight of 1.0. The limit values to produce oxygen were specified with a lower value of 27.72% and an upper value of 104.5%. Under these limits and conditions, the optimization of the adsorption process was carried out, and the results are depicted in Figure 8.

4. Model Application

The model predicted in the previous article suggested optimum values of pressure of 2.5 bar, the flowrate of 9.030 L·min^{-1}, and a

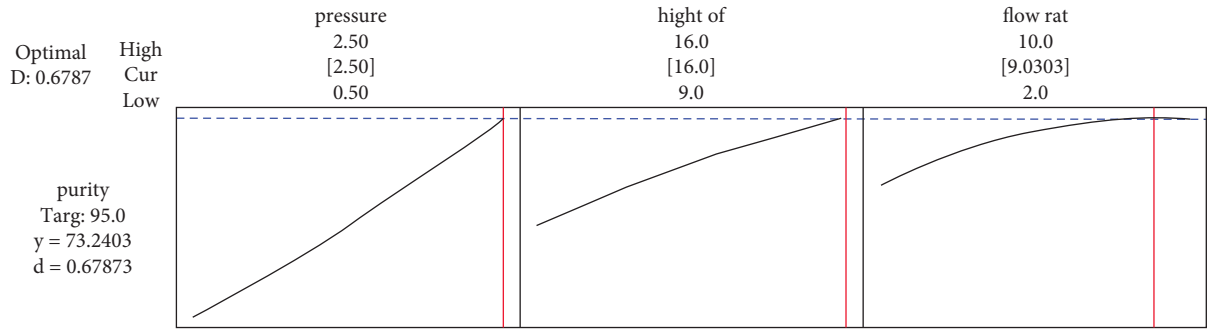

Figure 9: Optimum variables for maximum responding prediction.

packing height of 16 cm. These optimum conditions represented the extremes of the operating variables. If the pressure and the flowrate are kept constant, the packing height that is required to produce 95% oxygen purity could be computed by the model obtained. The amount of adsorbent needed would be a 20-cm-long column or 147 g of molecular sieve zeolite Li-LSX.

5. Conclusions

Oxygen production has been successfully synthesized by the adsorption process using zeolite Li-LSX. The results showed that increasing the pressure, the height of packing, and the flowrate led to increased O_2 purity. The Box–Behnken design has proven to be a beneficial and accurate methodology for optimizing nitrogen adsorption. The experimental data showed a good fit for the second-order polynomial model with an R^2 of 0.9892. The pressure mainly affected the purity, and the optimum conditions were 2.5 bar, 16 cm, and 9.030 $L{\cdot}min^{-1}$ flowrate, resulting in 73.2403% purity, which was very close to the experimental results. Increased N_2 adsorption selectivity can be achieved by increasing the amount of adsorbent material.

Data Availability

The data that support the findings of this study are included within the manuscript.

Conflicts of Interest

The authors declare that they have no conflicts of interest.

Supplementary Materials

The supplementary figures and tables are attached with the manuscript. (*Supplementary Materials*)

References

[1] R. R. Vemula, M. D. Urich, and M. V. Kothare, "Experimental design of a "snap-on" and standalone single-bed oxygen concentrator for medical applications," *Adsorption*, vol. 27, no. 4, 2021.

[2] A. Arora and M. M. F. Hasan, "Flexible oxygen concentrators for medical applications," *Scientific Reports*, vol. 11, no. 1, 2021.

[3] S. Qadir, D. Li, Y. Gu et al., "Experimental and numerical analysis on the enhanced separation performance of a medical oxygen concentrator through two-bed rapid pressure swing adsorption," *Industrial & Engineering Chemistry Research*, vol. 60, no. 16, pp. 5903–5913, 2021.

[4] L. He, M. Gao, F. Ning et al., "Ultralight, safe, economical, and portable oxygen generators with low energy consumption prepared by air-breathing electrochemical extraction," *ACS Applied Materials & Interfaces*, vol. 14, no. 24, pp. 28114–28122, 2022.

[5] A. A. Tishin, "Study of adsorption properties of zeolites NaX, CaA, and CaNaA in separation of air components," *Petroleum Chemistry*, vol. 60, no. 8, pp. 964–970, 2020.

[6] E. N. Ivanova, A. A. Averin, M. B. Alekhina, N. P. Sokolova, and T. V. Kon'kova, "Thermal activation of type X zeolites in the presence of carbon dioxide," *Protection of Metals and Physical Chemistry of Surfaces*, vol. 52, no. 2, pp. 267–272, 2016.

[7] A. A. Tishin and V. N. Gurkin, "Development of a mathematical model of molecular-selective gas transfer in a hybrid membrane-adsorption oxygen concentrator," *Journal of Physics: Conference Series*, vol. 1368, no. 4, Article ID 042043, 2019.

[8] E. I. Akulinin, F. N. Gladyshev, and S. I. Dvoretskii, "Advanced technologies and methods for creation of composite sorption-active materials for cyclic adsorption processes," *Vestnik Samarskogo Gosudarstvennogo Tekhnicheskogo Universiteta*, vol. 23, no. 1, pp. 85–103, 2017.

[9] Y. Wang, Y. An, Z. Ding, Y. Shen, Z. Tang, and D. Zhang, "Integrated VPSA processes for air separation based on dual reflux configuration," *Industrial & Engineering Chemistry Research*, vol. 58, no. 16, pp. 6562–6575, 2019.

[10] C. C. Chao, "Process for separating nitrogen from mixtures thereof with less polar substances," US4859217A, 1989.

[11] R. T. Yang, *Adsorbents: Fundamentals and Applications*, John Wiley & Sons, Inc, New York, NY, USA, 2003.

[12] C. W. Skarstrom, "Use of adsorption phenomena in automatic plant-type gas analyzers," *Annals of the New York Academy of Sciences*, vol. 72, pp. 751–763, 1959.

[13] N. Ayawei, S. S. Angaye, D. Wankasi, and E. D. Dikio, "Synthesis, characterization and application of Mg/Al layered double hydroxide for the degradation of congo red in aqueous solution," *Open Journal of Physical Chemistry*, vol. 05, no. 03, pp. 56–70, 2015.

[14] J. Ismail and A. Bansal, "Medical oxygen: a lifesaving drug during the COVID-19 pandemic—source and distribution," *Indian Journal of Pediatrics*, vol. 89, no. 6, pp. 607–615, 2022.

[15] C. Theivarasu and S. Mylsamy, "Removal of malachite green from aqueous solution by activated carbon developed from

cocoa (theobroma cacao) shell-a kinetic and equilibrium studies," *E-Journal of Chemistry*, vol. 8, no. s1, pp. S363–S371, 2011.

[16] A. Zirehpour, A. Rahimpour, M. Jahanshahi, and M. Peyravi, "Mixed matrix membrane application for olive oil wastewater treatment: process optimization based on taguchi design method," *Journal of Environmental Management*, vol. 132, pp. 113–120, 2014.

[17] *Coulson & Richardson's, Chemical Engineering*p. 605, 6th edition, Elsiever, Amsterdam, Netherlands, 1999.

[18] A. Srinivasan and T. Viraraghavan, "Oil removal from water by fungal biomass: a factorial design analysis," *Journal of Hazardous Materials*, vol. 175, no. 1–3, pp. 695–702, 2010.

[19] S. Demim, N. Drouiche, A. Aouabed, T. Benayad, M. Couderchet, and S. Semsari, "Study of heavy metal removal from heavy metal mixture using the CCD method," *Journal of Industrial and Engineering Chemistry*, vol. 20, no. 2, pp. 512–520, 2014.